Carbon Trends 17 (2024) 100424

Contents lists available at ScienceDirect

Carbon Trends

journal homepage: www.elsevier.com/locate/cartre

Exploration of graphitic carbon from crude oil vacuum residue

Ravi Dalsania [a,b,*], Hasmukh Gajera [a], Mahesh Savant [b]

[a] Reliance Industries Limited, Village Motikhavdi, Jamnagar 361140, Gujarat, India
[b] Department of Chemistry, Atmiya University, Rajkot, Gujarat 360005, India

ARTICLE INFO

Keywords:
ARA analysis
Characterization
^{1}H and ^{13}C NMR
Vacuum residue
Graphitic carbon

ABSTRACT

Preparation of graphitic carbon from low value refinery waste has captivated immense interest in past years owing to its low cost and abundant nature. Successful utilization of petroleum vacuum residue is a major challenge in the petroleum industry. In this study pyrolysis of vacuum residue fractions has been carried out for the preparation of graphitic carbon like material. The vacuum residue fractions were obtained from three different crude oils originated from Middle East, Canada and South America. The purity of the Aromatic, Resin and Asphaltene (ARA) fractions were confirmed using TLC-FID which denoted complete separation. The chemical composition were determined using elemental analysis and it revealed ARA fractions to be carbon rich regardless of its origin. Further, sulphur content was found to be high in ARA fractions from Heavy Crude oil (HCO). The degree of polymerization and molecular weight measured using GPC specify that asphaltene has high accumulation with high molecular weight compared with aromatic and resins. ARA derived carbon and heat-treated materials were analysed by TGA, XRD and Raman spectroscopy to study microstructural changes in formation of graphite like material. Thermogravimetric analysis of all ARA samples revealed the different decomposition stages for pyrolyzed, calcined and graphitized samples. The results of XRD demonstrated that the distance between the planes (d-spacing) is above 3.35 Å for all high temperature treated ARA derived carbon materials irrespective of its origin, indicating formation of graphite like structure. In Raman analysis, the nature and intensity of G and D bands evolution during each step of pyrolysis is supporting XRD results for formation of highly ordered graphitic carbon material. Furthermore, understanding feed quality has direct influence on high efficiency, low costs and sustainability, the major issues for oil refinery business.

1. Introduction

Oil reserves play a vital role in uplifting overall economy and hence petroleum is a key element of modern civilization. Its constant demand has increased the cost of refinery in world. The refineries major cost comes from crude oil procurement. Investigating innovative method to refine heavy oil to highly sought light oil is one promising way to cut down refinery costs. Though there are sophisticated methods a clear knowledge is still not achieved to understand the elaborate chemistry of petroleum. In general, it is understood that a diverse oil characterization is required to confront the challenge of crude oils complex nature [1]. In this regard numerous characterization studies on bulk physical and chemical properties; and on SARA analysis for crude oil have attracted more attention [2–5].

GPC is a common method for the estimation of molecular weight distributions of asphaltene [6]. Gel permeation chromatography of the crude oil provides the benefit of short analysis time and offers reliable data on molecular weight distribution and its evaluation [7]. N. Alawani et al. [1] have used gel permeation chromatography to obtain chemically well-defined fractions on the separation of crude oils. B. Azinfar et al. [8] used both simulated distillation and GPC for a better insight of the molecular weight distributions of complex mixtures. Likewise, fractionation technique with combined separation power of TLC and a universal detector FID accompanied with the simplicity, short duration and low demand for hazardous solvents has made TLC-FID superior for the investigation of a wide spectrum of organic compounds [9,10]. TLC-FID is used extensively for measuring aromatic and saturated hydrocarbons, and asphaltene/resin extracts in solvent fractions of crude oils, petroleum source rocks, and reservoir rocks [11,12].

Furthermore, carbon, hydrogen, nitrogen, sulfur and oxygen

Abbreviation: ARA, aromatic resin and asphaltene; EHCO, extra heavy crude oil; LCO, light crude oil; HCO, heavy crude oil; TLC-FID, Thin layer chromatography and flame ionization detection; GPC, Gel Permeation Chromatography; FT-ICR, Fourier transform ion cyclotron resonance mass spectrometry.

* Corresponding author.
E-mail addresses: ravi.dalsania@ril.com (R. Dalsania), Hasmukh.Gajera@ril.com (H. Gajera).

https://doi.org/10.1016/j.cartre.2024.100424
Received 12 August 2024; Received in revised form 4 November 2024; Accepted 4 November 2024
Available online 5 November 2024

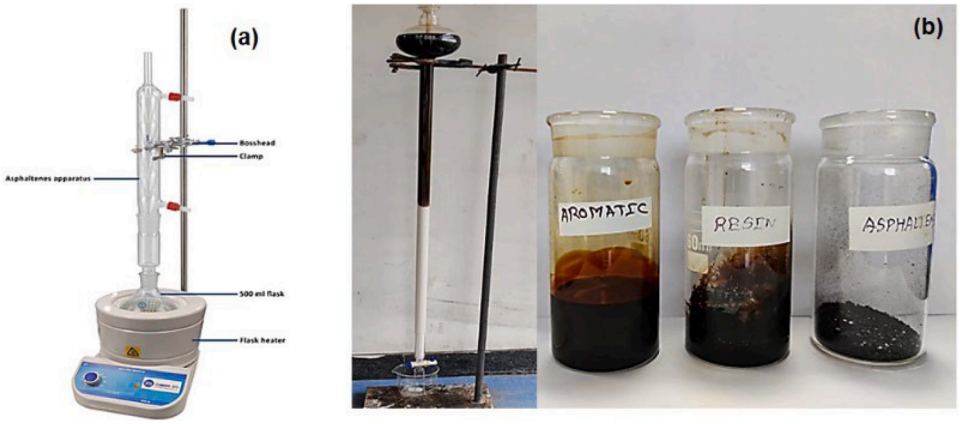

Fig. 1. a) Schematic of Soxhlet extractor for asphaltene separation and b) ARA fraction characterized in this study.

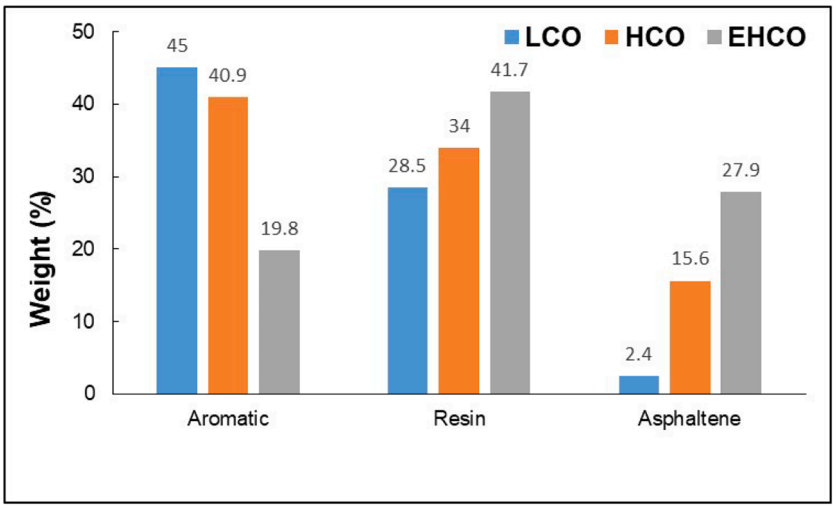

Fig. 2. Weight distribution of aromatic, resin and asphaltene (ARA) fractions for the three vacuum residues.

Table 1
Properties of vacuum residue fractions extracted from the crude oils under investigation.

Characteristics	LCO	HCO	EHCO
Pour point (wt. %)	60	118	139
CCR (wt. %)	22.7	29.3	35.1
Density (g/ml)	1.0339	1.0801	1.0856
Total carbon (wt. %)	83.8	82.87	85.06
Total Hydrogen (wt. %)	11.2	9.38	10.04
Total Nitrogen (wt. %)	0.66	0.77	1.01
Total Sulphur (wt. %)	3.68	6.17	3.54
Total Oxygen (wt. %)	0.66	0.81	0.35
Heteroatoms (wt. %)	5.00	7.75	4.90
C/H ratio	7.48	8.83	8.47
Total Metals (wt. ppm)	137	718	1464

(CHNSO) are few of the usually identified elements in crude oil which influence the fuel product properties. For example, sulfur content is one of the significant corrosive media in crude oil [13]. Similarly, nitrogen-containing compounds create problem such as deactivation and inhibition of acid catalyst, corrosion related to acid-base pair, and metal complexation [14]. Therefore, it is a common practice of elemental analysis for determination of CHNSO content in petroleum products. In the same way organometallic complexes are formed by the presence of metallic particles which tends to be significant precursors in the asphaltenes precipitation during the refining processes. ICP-OES is broadly implemented in the petrochemical industry for the examination of trace elements during refining of crude oil [15,16]. Ash content a measure of inorganic impurities in the crude oil which affects boiler efficiency is also determined by ICP-OES [17,18].

In recent years, mass spectrometry serves as a basic approach for the accurate analysis of mass and structure of crude oil components [19–21]. J.M. Santos et al. [19] have shown SARA fractionation analysis by FT-ICR MS has allowed the individual fraction and selective chemical of the crude oil components characterization. Likewise, P. Juan et al. [20] have established the usage of FT-ICR MS as a potential tool in combination with supercritical fluid extraction fractionation to study molecular composition of the vacuum residue. Similarly, Z. Farmani et al. [21] have gained a clear image of the neglected fractions in crude oil studies and the saturate fraction by ultrahigh resolution mass spectrometry. Due to the occurrence of significant amount of compounds in crude oil, various ionization methods such as atmospheric pressure chemical ionization, electrospray ionization are employed for complex mixture analysis [22,23]. API- MS delivers option to handle the complex nature of crude oil by grouping compounds on the basis of heteroatom content, and designating molecular formulae [24].

In the same manner nuclear magnetic resonance and fourier transform infrared spectroscopy are utilized widely for the compositional inspection of crude oil. FTIR has been applied broadly for the structural determination of asphaltene [25–27]. M. Asemani et al. [27] performed geochemical correlation of different oil samples from four oil fields by applying FTIR spectroscopy to identify and relate asphaltene structures.

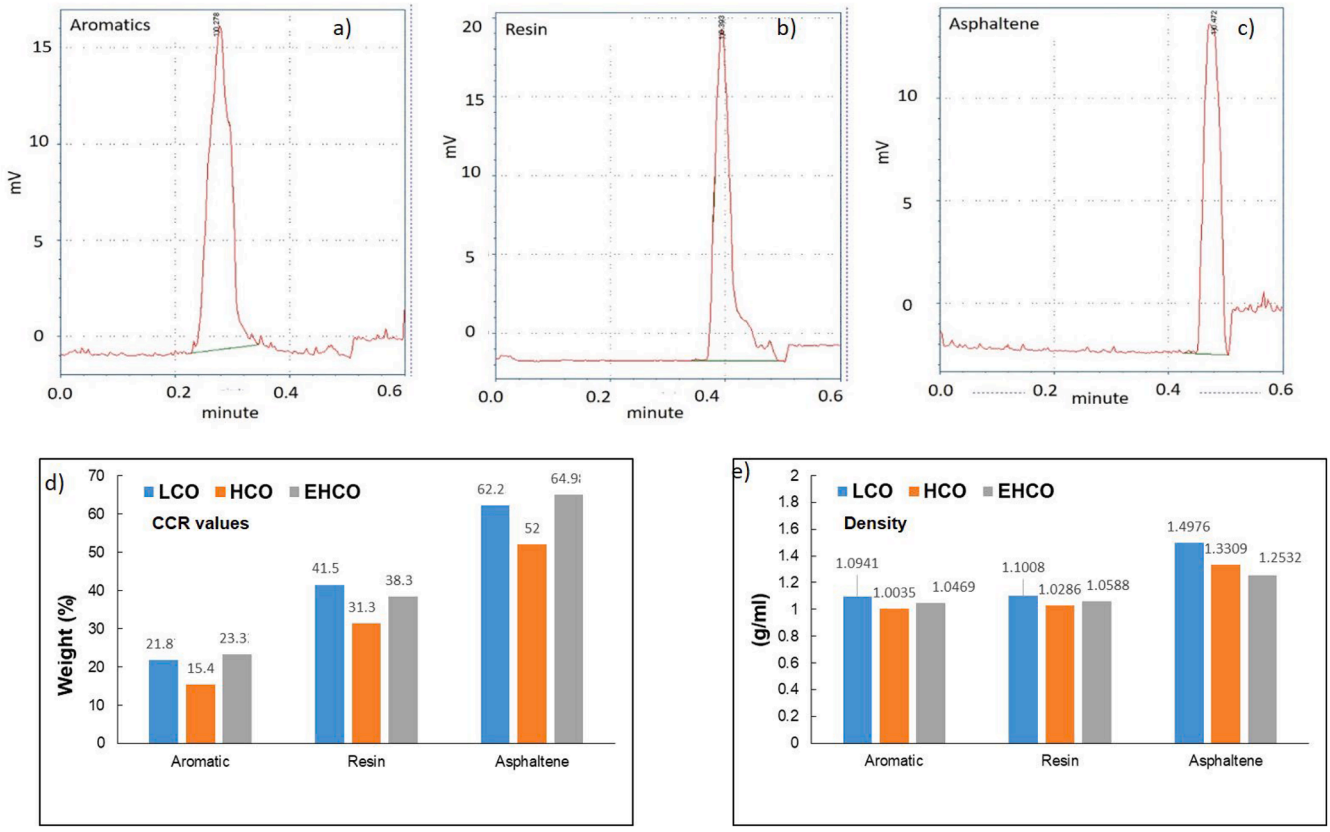

Fig. 3. TLC-FID chromatograms of the isolated a) aromatic, b) resin and c) asphaltene fractions, d) Conradson carbon residue prediction and e) density chart of ARA analysis.

Table 2
Origin based elemental analysis for extracted aromatic, resin and asphaltene.

Elemental Analysis	AROMATIC			RESIN			ASPHALTENE		
	LCO	HCO	EHCO	LCO	HCO	EHCO	LCO	HCO	EHCO
Total Carbon (wt. %)	85.24	83.11	85.41	84.91	82.88	85.09	84.51	82.20	86.71
Total Hydrogen (wt. %)	10.97	9.86	9.91	9.96	9.00	9.52	8.91	7.38	7.58
C/H ratio	7.77	8.43	8.62	8.53	9.21	8.94	9.48	11.14	11.44
H/C ratio	0.12	0.12	0.10	0.12	0.11	0.11	0.11	0.09	0.09
Total Nitrogen (wt. %)	0.41	0.39	0.72	0.97	1.09	1.32	1.56	1.36	1.65
Total Sulphur (wt. %)	2.7	5.78	3.18	3.06	6.25	3.34	3.53	8.34	3.97
Total Oxygen (wt. %)	0.61	0.86	0.78	1.10	0.78	0.73	1.49	0.72	0.09
Heteroatoms (wt. %)	3.72	7.03	4.68	5.13	8.12	5.39	6.58	10.42	5.71

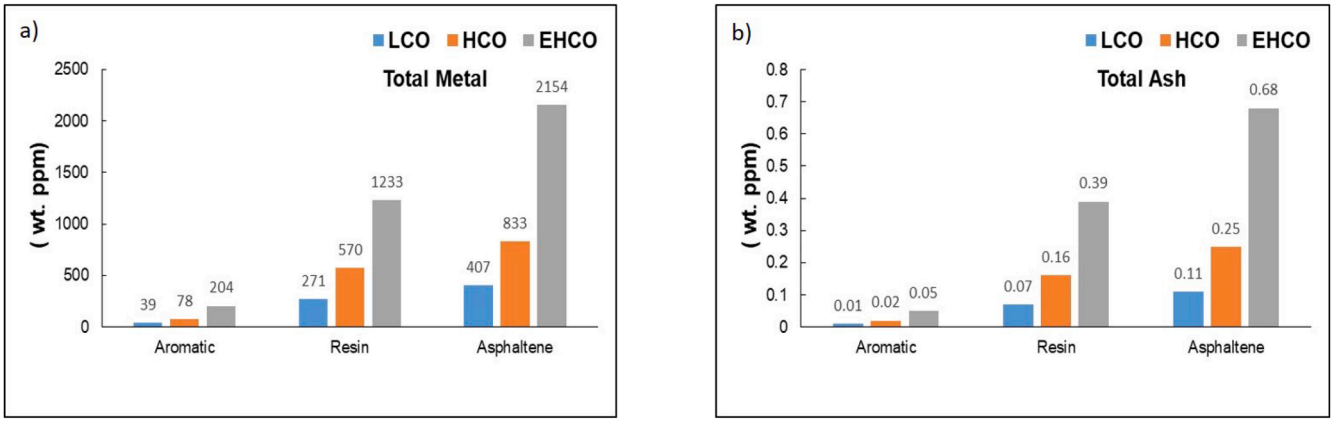

Fig. 4. Plot showing total metal and ash content in origin based ARA fractions.

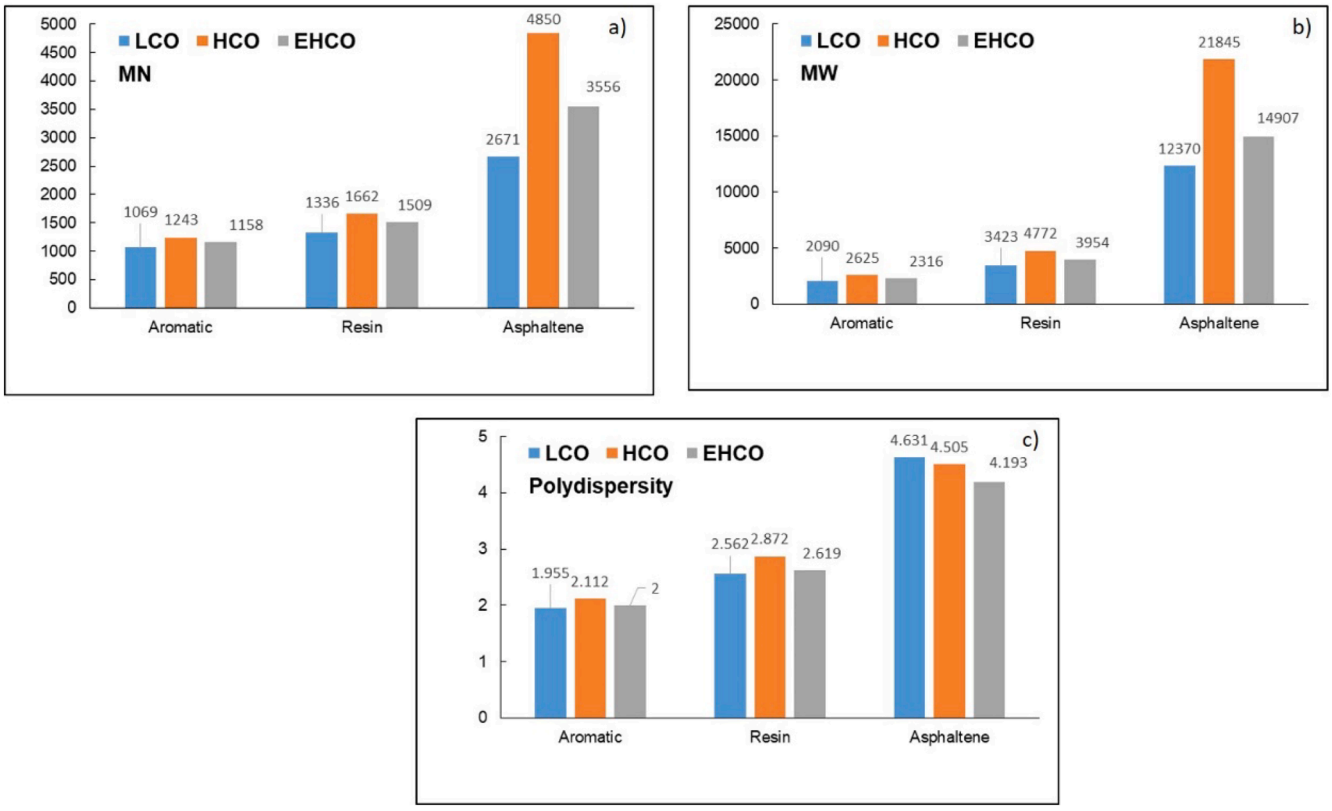

Fig. 5. Average molecular weight and polydispersity values by GPC.

Table 3
^{1}H NMR protons distribution of ARA fractions.

NMR	Types	δ position	AROMATIC			RESIN			ASPHALTENE		
			LCO	MCO	HCO	LCO	MCO	HCO	LCO	MCO	HCO
1H NMR	Hal; γ	0,1–1,1	18,08	22,59	21,63	17,14	18,39	17,98	33,42	17,15	22,25
	Hal; β	1,2–2,1	47,65	55,03	44,54	47,00	52,01	45,55	37,83	55,50	56,07
	Hal; α	2,2–4,0	18,00	10,82	23,29	22,59	18,68	20,70	13,35	17,81	13,29
	Har mono aromatic rings	6,0–7,1	7,87	6,22	5,16	5,03	4,99	4,96	9,22	4,65	3,46
	Har of di, tri and tetra aromatic rings	7,3–9,0	8,39	5,34	5,38	8,23	5,94	10,80	6,18	4,89	4,94
	Total aliphatic hydrogen	0,4–4,0	83,73	88,44	89,46	86,73	89,08	84,23	84,60	90,46	91,61
	Total aromatic hydrogen	6,0–9,0	16,26	11,56	10,54	13,26	10,93	15,76	15,40	9,54	8,40

Table 4
^{13}C NMR protons distribution of ARA fractions.

NMR	Types	δ position	AROMATIC			RESIN			ASPHALTENE		
			LCO	MCO	HCO	LCO	MCO	HCO	LCO	MCO	HCO
^{13}C NMR	Methyl of carbon to aliphatic or alkyl chain	10–20	11,51	13,24	3,34	12,79	8,79	8,40	7,48	13,08	4,76
	Methylene of carbon to aliphatic or alkyl chain	20–25	11,51	8,68	13,04	9,30	9,56	13,20	7,48	8,41	9,52
	Methylene group attached to aromatic ring	25–40	9,71	36,53	42,14	41,67	49,35	50,80	33,18	35,98	71,43
	CH of aromatic compounds	110–160	67,27	41,55	41,47	36,24	32,30	27,60	51,87	42,52	14,29
	Total aliphatic carbon	10–40	32,73	58,45	58,52	63,76	67,70	72,40	48,14	57,47	85,71
	Total aromatic carbon	110–160	67,27	41,55	41,47	36,24	32,30	27,60	51,87	42,52	14,29

Table 5
Yield of carbon at different stages of pyrolysis.

SAMPLE	AROMATIC			RESIN			ASPHALTENE		
	LCO	HCO	EHCO	LCO	HCO	EHCO	LCO	HCO	EHCO
Green Carbon	21.9	15.4	23.3	41.5	31.4	38.4	62.3	52.0	65.0
Calcined Carbon	85.0	79.4	82.4	83.9	82.4	80.4	75.7	75.6	71.5
Graphitized carbon	96.2	96.0	99.3	92.5	95.8	97.7	94.5	99.5	98.0

Table 6
Elemental proportions of carbon samples.

Origin	Sample	Total Carbon	Total Hydrogen	Total Nitrogen	Total Sulphur	Total Oxygen	Total Heteroatoms
Aromatic LCO	Green	89.39	2.43	0.69	5.39	2.10	8.18
	Calcined	98.21	0.07	0.21	1.51	0.00	1.72
	Graphitized	99.99	0.00	0.01	0.00	0.00	0.01
Aromatic HCO	Green	88.59	2.68	1.26	5.40	2.07	8.73
	Calcined	97.94	0.03	0.31	1.72	0.00	2.03
	Graphitized	99.99	0.00	0.01	0.00	0.00	0.01
Aromatic EHCO	Green	91.02	2.82	1.45	3.60	1.11	6.16
	Calcined	94.79	0.03	0.32	2.31	2.55	5.18
	Graphitized	99.99	0.00	0.01	0.00	0.00	0.01
Resin	Green	88.17	2.10	1.18	6.69	1.86	9.73
LCO	Calcined	96.82	0.04	0.34	2.81	0.00	3.14
	Graphitized	99.99	0.00	0.01	0.00	0.00	0.01
Resin	Green	88.36	2.55	1.98	4.03	3.08	9.09
HCO	Calcined	96.38	0.03	0.51	2.74	0.35	3.60
	Graphitized	99.99	0.00	0.01	0.00	0.00	0.01
Resin	Green	88.36	2.55	1.98	4.03	3.08	9.09
EHCO	Calcined	96.38	0.03	0.51	2.74	0.35	3.60
	Graphitized	99.99	0.00	0.01	0.00	0.00	0.01
Asphaltene	Green	87.60	2.01	1.57	7.02	1.80	10.39
LCO	Calcined	95.47	0.04	0.19	2.05	2.25	4.49
	Graphitized	99.99	0.00	0.01	0.00	0.00	0.01
Asphaltene	Green	82.27	1.77	2.50	7.83	5.64	15.97
HCO	Calcined	94.61	0.02	0.35	3.01	2.02	5.38
	Graphitized	99.99	0.00	0.01	0.00	0.00	0.01
Asphaltene	Green	87.19	2.16	2.36	4.69	3.60	10.65
EHCO	Calcined	94.93	0.01	0.43	3.48	1.15	5.06
	Graphitized	99.99	0.00	0.01	0.00	0.00	0.01

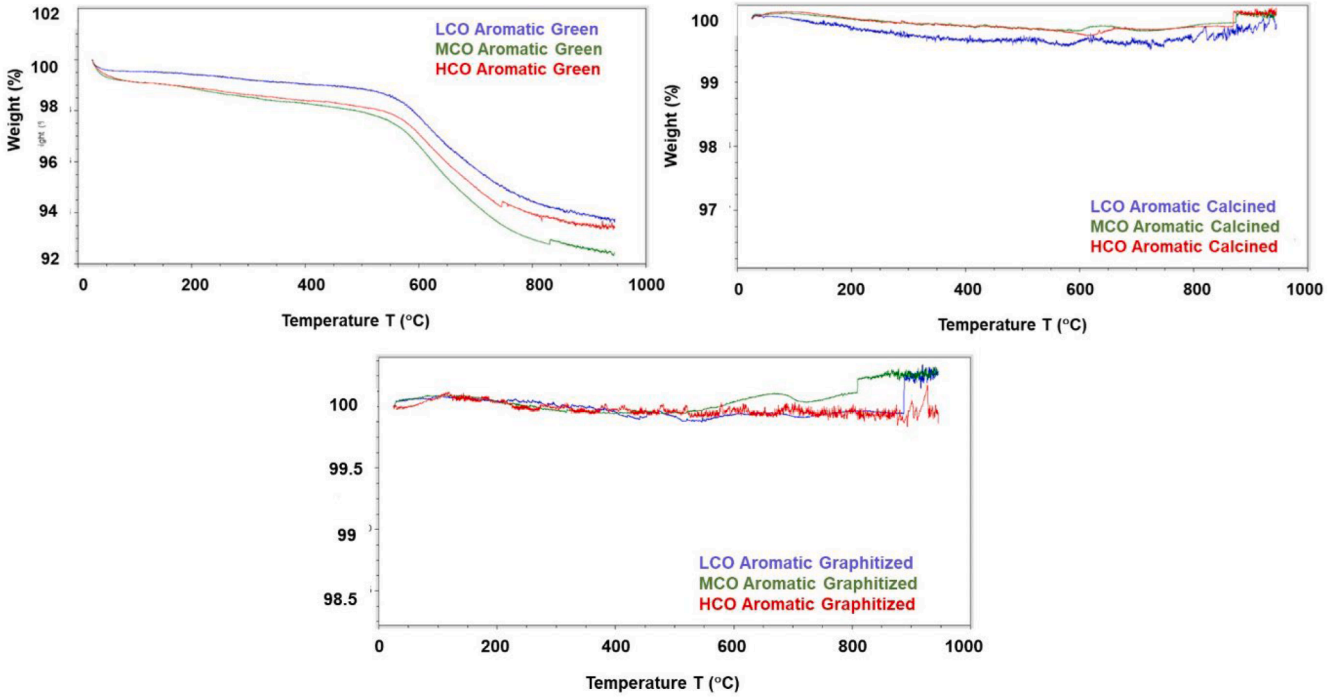

Fig. 6. TGA analysis of green, calcined and graphitized carbon from origin based ARA fractions.

S. B. Yang et al. [28] employed FTIR and data-driven methods to anticipate crude oil properties. In similar way, NMR studies furnish essential details on organic matter functional groups [29–31]. It also indicates the source rock sedimentary surroundings, and thermal maturity thus has distinctive advantage in geochemical assessment of crude oil [29]. The Low-field nuclear magnetic resonance based method has realistic utility like non-destructive, require minimum sample without hazardous solvents, analysis cost is economical, analysis is quick, whole method workflow is straightforward and easy to perform physical property determination [30]. Rakhmatullin et al. [31] present the possibility of ^{13}C NMR spectroscopy for the quick analysis of heavy crude oil from physical characteristics to the arrangement of functional groups. It additionally highlights the capability of NMR to study both systematically and empirically the elemental configuration along with molecular composition of organic materials, its fractions, and aspired products. However, sophisticated analytical procedures are still required to enhance the performance of refinery conversion processes.

Moreover it is established that the chemical characteristics of crude oil vary based on its origin. Besides refinery usually use blend of crude oils [32]. Hence various groups have shown interest to study the

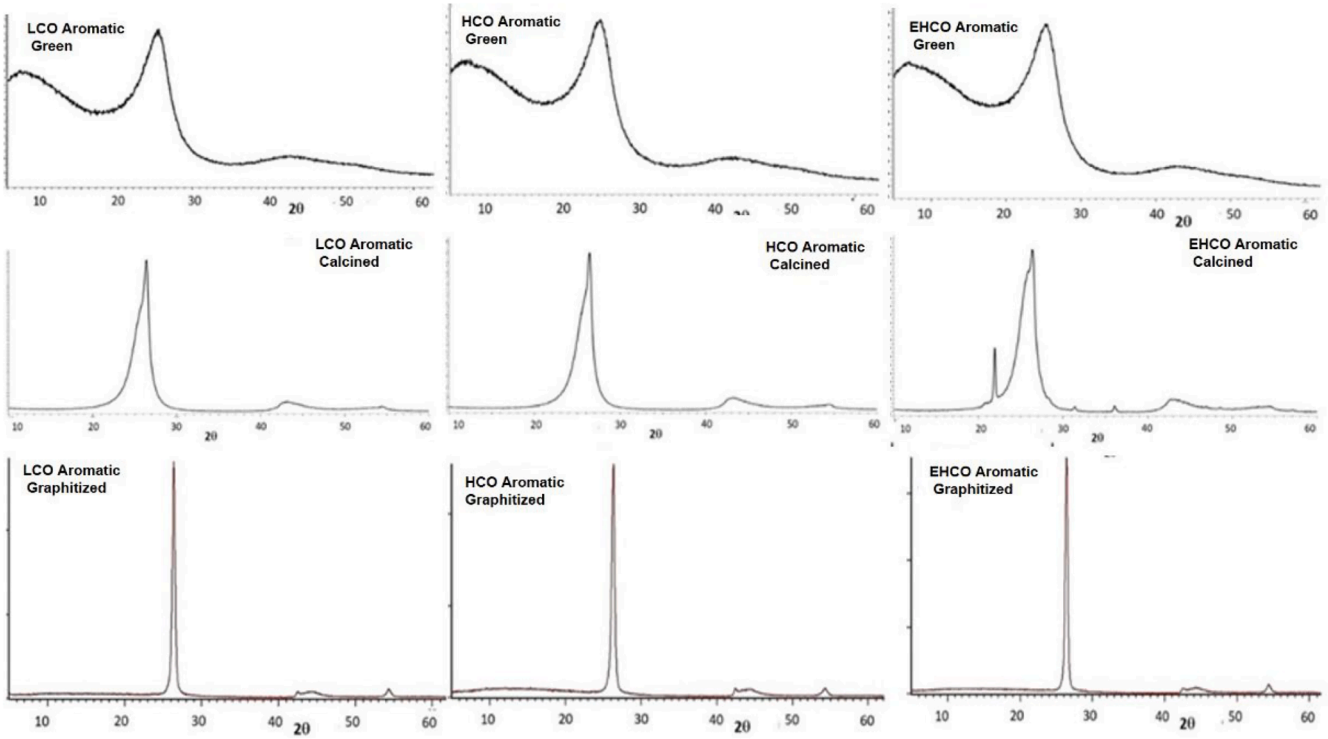

Fig. 7. XRD pattern of green, calcined and graphitized samples from aromatics.

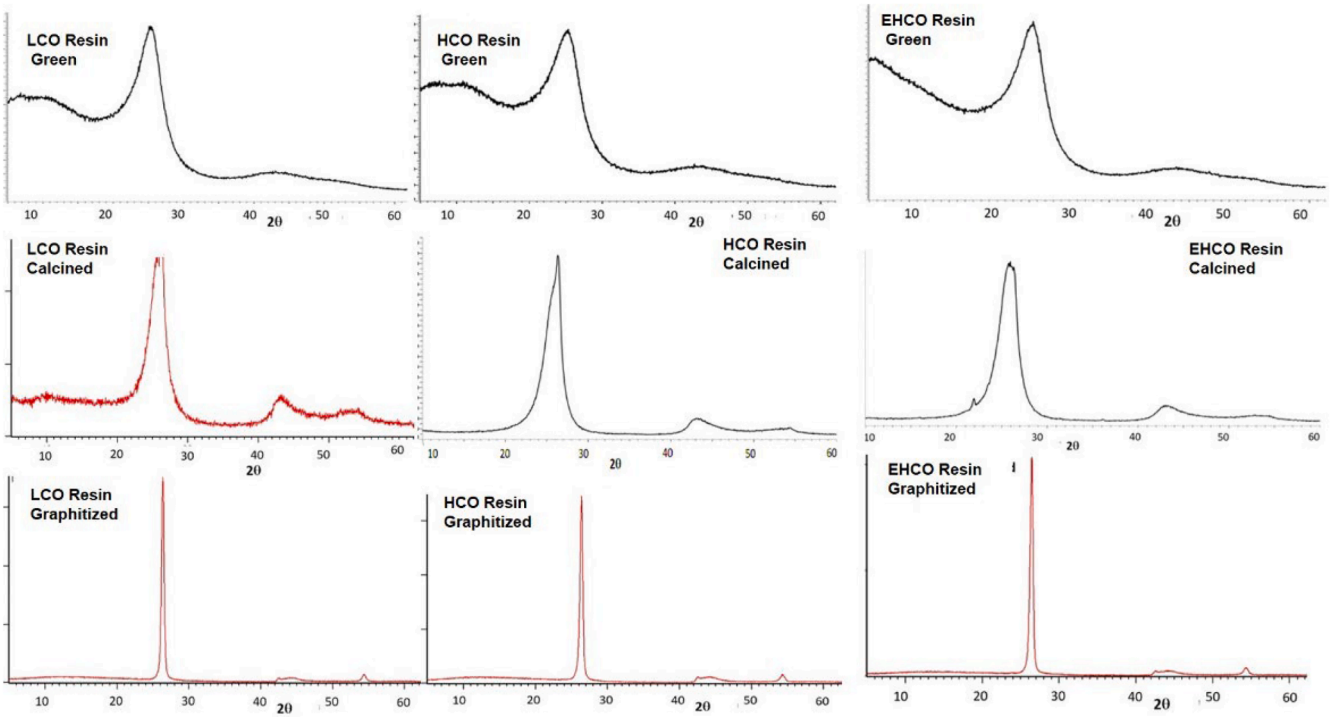

Fig. 8. XRD pattern of green, calcined and graphitized samples from resins.

characteristics of crude oil from different origin [33–35]. A. B. Garmarudi et al. [33] used infrared spectrometry and chemometrics to successfully classify crude oils based on its origin. Similarly, O. Galtier et al. [34] utilized mid-infrared spectroscopy to classify crude petroleum oils according to their geographical origins. Likewise M. Salehzadeh et al. [35] carried profound investigation of light, medium and heavy oil asphaltenes and observed excess hydrogen content and hydrogen/carbon atomic ratio in heavy oil asphaltene. Nevertheless, there is a significant anticipation for origin based studies on crude oil.

Additionally, in recent years there are few reports on effective use of petroleum vacuum residue as a raw material to convert into high value carbon based materials. Currently, with the constant growth in concern over management of natural resources the petrochemical industry have difficulties in efficiently managing petroleum vacuum residue. Besides,

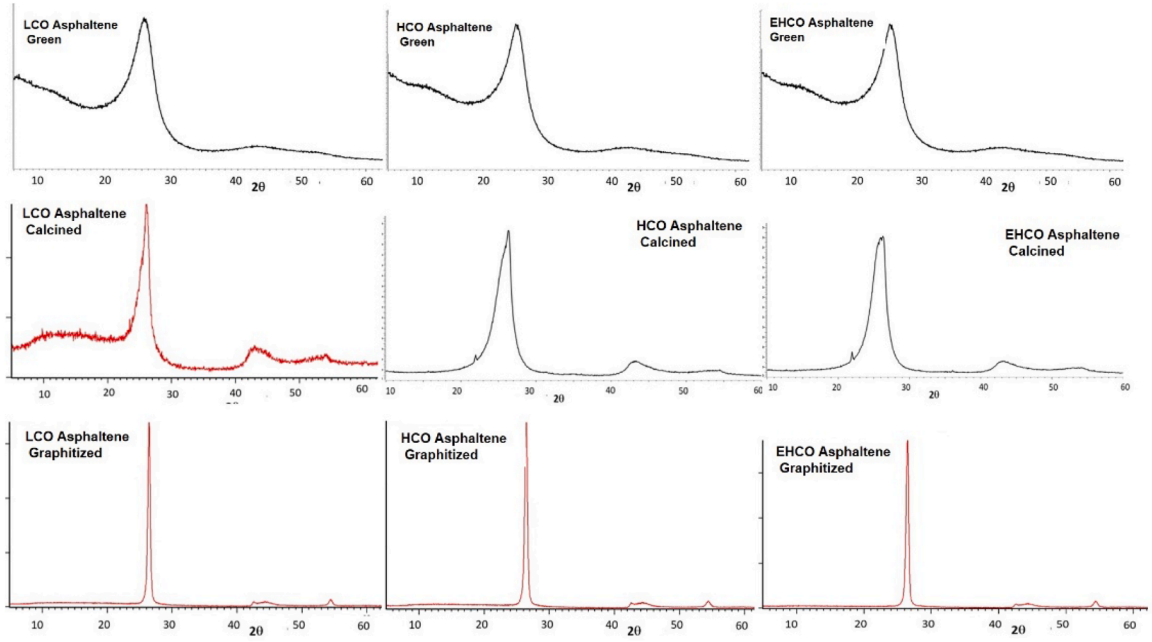

Fig. 9. XRD pattern of green, calcined and graphitized samples from asphaltenes.

Table 7
Data obtained for XRD analysis.

Sample	Origin	AROMATIC			RESIN			ASPHALTENE		
		d-spacing (A°)	Lc (A°)	La (A°)	d-spacing (A°)	Lc (A°)	La (A°)	d-spacing (A°)	Lc (A°)	La (A°)
Green	LCO	3.515	21.30	16.90	3.518	22.60	21.90	3.505	22.80	18.10
Calcined		3.380	8.022	4.165	3.386	7.868	4.487	3.47	3.16	3.53
Graphitized		3.382	20.279	43.062	3.379	19.673	43.004	3.372	19.23	34.59
Green	HCO	3.528	20.70	19.70	3.538	20.90	24.10	3.524	19.90	25.30
Calcined		3.377	8.290	4.332	3.381	6.924	3.865	3.387	6.09	3.89
Graphitized		3.387	17.814	45.672	3.387	18.744	39.774	3.371	16.75	34.89
Green	EHCO	3.522	21.20	19.80	3.513	21.40	20.80	3.507	24.00	21.80
Calcined		3.380	7.581	3.541	3.392	5.432	4.115	3.389	5.87	3.54
Graphitized		3.380	24.579	36.645	3.362	20.712	33.085	3.371	18.49	38.04

the effective utilization of high value added petroleum vacuum residue is also economical. X. Zhai et al. [36] fabricated Fe,N-codoped porous carbon-embedded Fe_3C nanoparticles from petroleum vacuum residue for highly efficient oxygen reduction. For Li-ion batteries anodic material, J. L. Tirado et al. [37] carried co-pyrolysis of petroleum residue to obtain Tin-carbon composites and SnO_2. Furthermore H. Chao et al. [38] reports of carbon with porous structure from vacuum residue for its implementation in Lithium ion capacitors.

The purpose of the research is to carry out an extensive characterization for aromatic, resin and asphaltene fractions from vacuum residue distillate of light, heavy and extra heavy crude oil. Furthermore, the purpose is also to convert ARA fractions into graphitic carbon like material and study co-relation of each type of vacuum residue on conversion of graphitic carbon material. For which heat treated samples at all stages are analysed to understand structural changes using TGA, XRD and Raman spectroscopy. All results are discussed in details in this article.

2. Materials and methods

2.1. Studies on vacuum residue and ARA analysis

2.1.1. Materials

Crude oils with distinct characteristics were selected and tested from three separate origins: Middle East, Canada and South America. Based on their American Petroleum Institute values they are referred as Low (Middle East, API - 33.4), Heavy (Canada, API - 21.4) and Extra Heavy (South America, API - 9.5) crude oil throughout the study. The Low (LCO), Heavy (HCO) and Extra Heavy (EHO) exhibited Conradson Carbon Residue values of 5.1, 9.5 and 12.9, respectively.

2.1.2. Methods

To estimate the yield of fractions regular test methods for distillation of crude petroleum (ASTM D2892) and heavy hydrocarbon mixtures (ASTM D5236) were done. The resulting vacuum residues were considered as raw materials for this study. The determination of asphaltene in vacuum residue was carried out by following ASTM D6560 (Fig. 1a). The remaining maltenes were passed through column bed prepared by activated, alumina oxide with mesh size 100 and silica gel of FIA grade. The glass column length was 1150 mm, internal diameter 15 mm and bulb capacity 500 ml for 10 g sample weight. The saturates were obtained as first fraction which is soluble in n-heptane. Aromatic fraction was obtained next by addition of toluene in bulb. Finally, resin fraction was obtained by adding a mixture of toluene and methanol in 1:1 ratio. The fraction solvents were evaporated to get the pure SAR fractions. The ARA fractions studied in this study are represented in Fig. 1b.

The purity of the fractions isolated using the above described method was measured using TLC-FID on a latroscan MK-6S system. The hydrogen flow rate of the FID was 160 mL/min; the air flow rate was 2

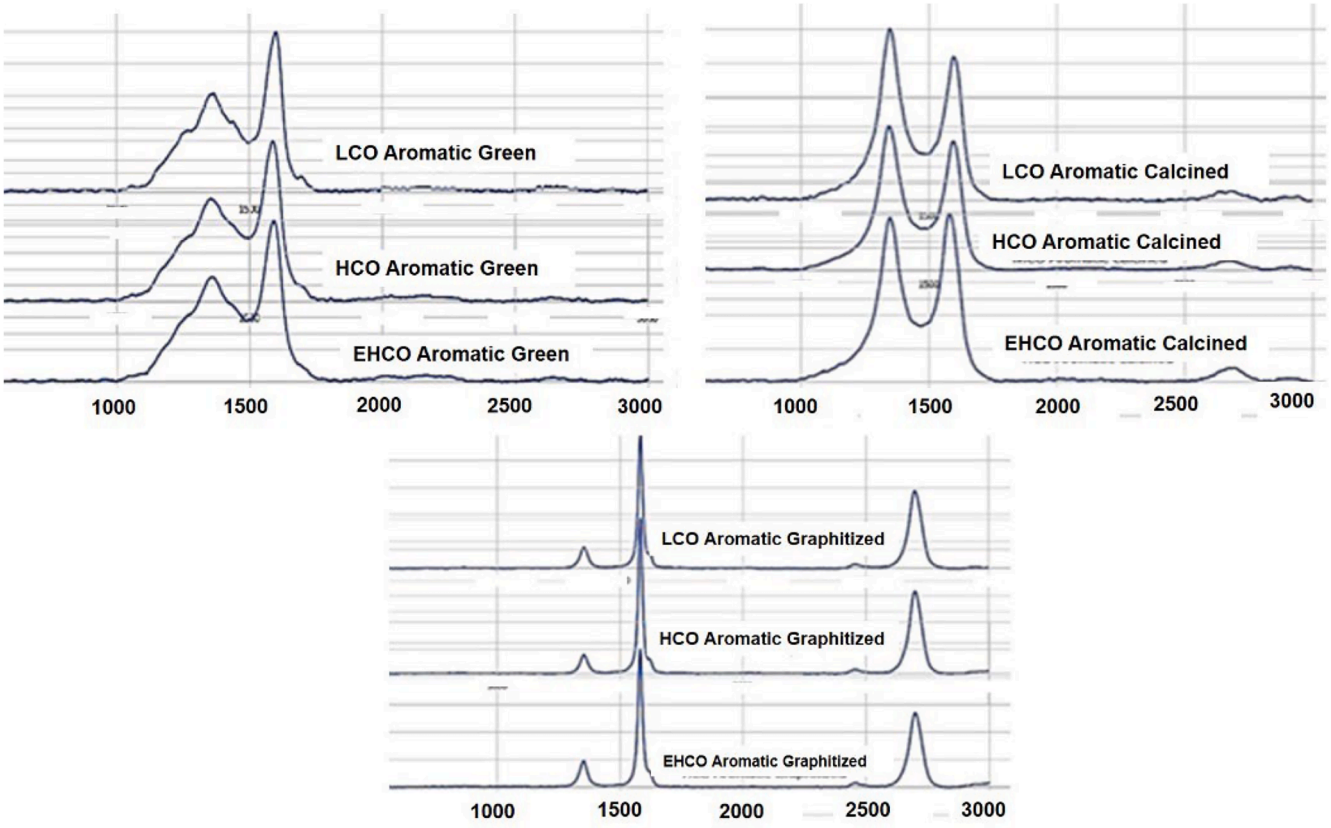

Fig. 10. Raman spectra of green, calcined and graphitized carbon of origin based aromatics.

L/min. A solution of approximately 1 % wt. /vol. of material in dichloromethane was prepared, of which 1 μL drop was spotted on silica coated chroma rod. It was followed by drying at 80 °C in oven for 5 min after which the chromarod was eluted sequentially. The first chamber filled with n-hexane for saturates at 100 mm height.

However, the saturate were eliminated from this study due to their low carbon yield % following pyrolysis at 500 °C for 10 min. Second, it was heated once again at 80 °C for 5 min with known quantity of toluene for aromatic at 50 mm height was eluted. Finally for the last stage heating was carried for 10 min at 80 °C, chamber filled with methanol and DCM mixture for resin at 25 mm height was eluted. The data were collected with SIC-480 II software. This procedure was repeated for ARA fractions from different origin crude oil. ASTM D4530 method was used for the determination of the amount of carbon residue in ARA fraction. The relative density of the ARA fractions were measured by using pycnometer.

The CHNSO content was determined using the Elementary Vario Macro CUBE instrument. A known quantity of the sample was placed into a combustion tube at a temperature of 1150 °C. Under these circumstances, CHNS underwent quantitative conversion to their respective gases, namely CO_2, H_2O, NO_X, and SO_X. This conversion occurred during sample combustion at 850 °C in an oxygen-rich environment. The resulting gases were then directed into the reduction tube via a U-tube, where impurities such as excess oxides and halides were eliminated using copper and silver metals. Nitrogen content was directly measured using a TCD detector operating at 240 °C. Pure elemental oxide gases were trapped in a specific column and subsequently released at a designated temperature for analysis by the TCD detector, with helium serving as the carrier gas. Verification and calibration were conducted using various standards with different concentrations. Elemental analyses were performed on the VR sample and its fractions of ARA (Aromatic, Resins, and Asphaltene). In this process, samples weighing between 25 and 50 mg were prepared with double the quantity of tungsten oxide and then injected directly into the column using an auto sampler. The instrument's operational range spanned from 0 to 100 %, with a minimum detection limit of 100ppm.

Metal and ash content in crude oil were determined by inductively coupled plasma optical emission spectrometry (ICP-OES). Perkin Elmer optima 8300 model with sulphur chemiluminescence detector (SCD) was employed. The carrier gases were argon and oxygen. 0.2 to 0.25 gm samples were dissolved in an industrial solvent, decalin. Diluted samples were carried through peristaltic pump, samples and argon were mixed in nebulizer and made an aerosol. This aerosol and extra oxygen mixed in plasma tube generated plasma. These charged elements photon passed through photon multiplier tube and emitted the energy at the end of path. Emitted energy covert in electric signal in detection system. Minimum detection limit of the detector is 0.1 ppm.

The 60 mg samples were diluted in 5 mL tetrahydrofuran (THF). GPC analysis was performed using a Perkin Elmer Turbo matrix-40 instrument with PLgel mixed-b columns packed with 5 μm polystyrene gel beads with microporous stationary phase. The column length and diameter 300 * 7.5 mm with the flow rate of 1 mL min^{-1} for a total run time of 15 min was followed. Refractive index detector was used. Polystyrene standards were used to calibrate for relative M_W and M_N.

Mass analysis was conducted on a Waters Alliance e2695 separations module with QDa detector. The samples were prepared by weighing approximately 0.2 g sample dissolved in 250 ml toluene. The injection volume was 10 μL, total run time of 1 min. These samples were ran and recorded the data between 100 and 1000 Dalton mass and instrument limit is 50 to 1200 Dalton. The ^{1}H NMR and ^{13}C NMR spectra acquisition were obtained on a Bruker Biospin Avance III 400 MHz liquid state NMR spectrometer along with 5 mm Broad Band observed probe with gradient coil along Z axis. The samples were prepared by diluting samples in deutered chloroform ($CDCl_3$) solvent. Spectra were recorded using 16 scans, top spin 2.1 and the number of scans was 4000.

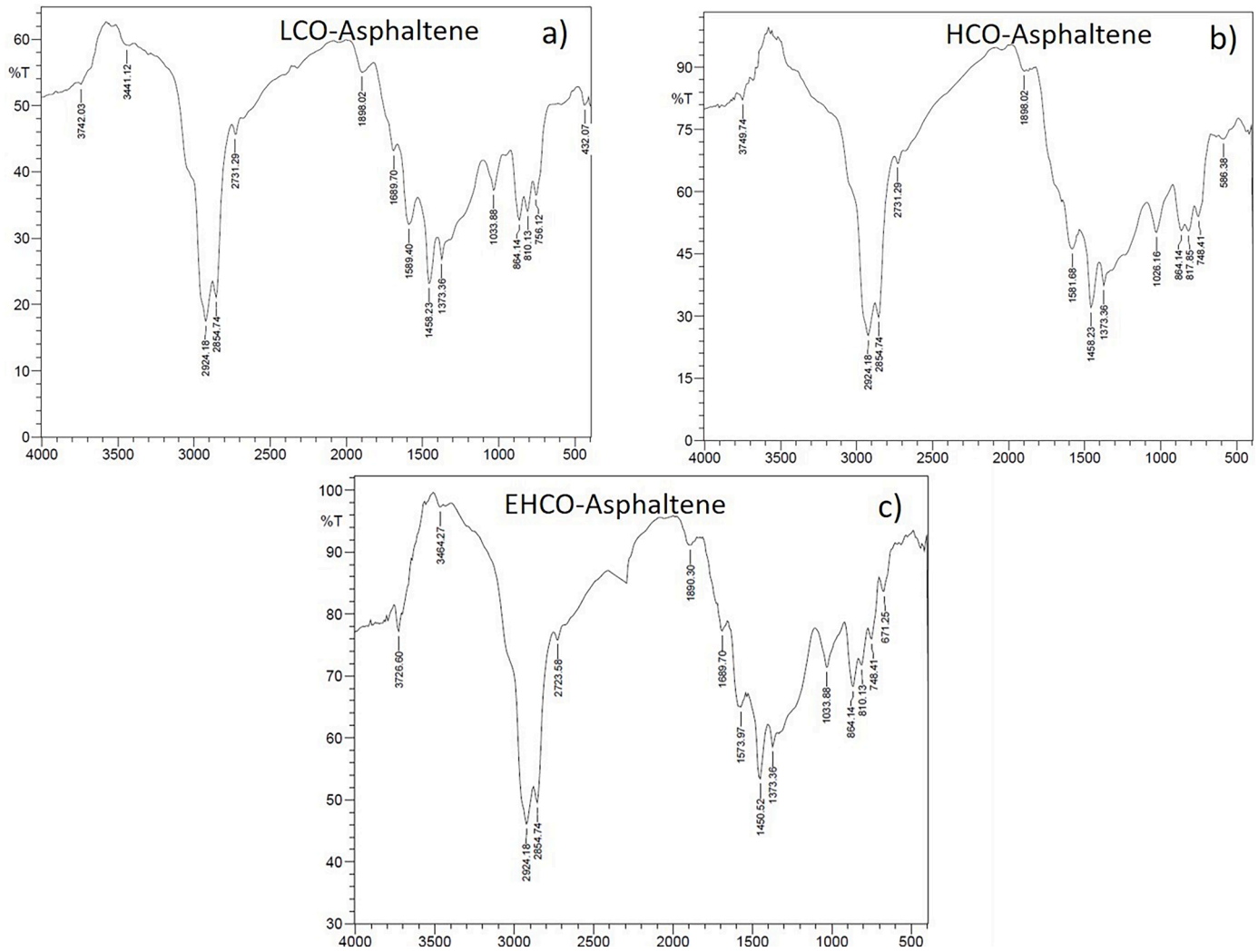

Fig. 11. FTIR spectra of the origin based asphaltenes.

2.2. Preparation of graphitic carbon like material

2.2.1. Materials

Aromatic, resin and asphaltene (ARA) fractions from three different vacuum residues (Light Crude oil, Heavy Crude oil and Extra Heavy Crude oil) were used as a raw material for preparation of green coke for this study.

2.2.2. Methods

The raw materials were pyrolyzed at 500 °C for 10 min under inert atmospheric condition as per ASTM D4530 resulting in the formation of green carbon. The obtained green carbon samples were further heat treated in two step, followed by heating at 900 °C with heating rate of 10 °C and 1350 °C with rate of 5 °C and held for 30 min and 5 hr respectively to produce calcined carbon. This was done to remove all volatile matters for further processing to get graphitized carbon. Graphitization was done at 2800 °C with heating rate of 15 °C and held for 2 hr.

The Raman spectra were recorded in Confocal Raman Microscope (LabRAM HR Evolution, HORIBA Scientific, Jobin Yvon Technology) at ambient temperature using the 532 nm laser in the wavenumber range 200–3000 cm^{-1}. The number of accumulations was 5 with time 2 s and the spectra were baseline corrected with the LabSpec6 software program. Multiple measurements were performed on powder of each individual sample and averaged spectra was represented. XRD measurements have been done on Panalytical's X'Pert Pro instruments. The radiation source used is Cu K-alpha and nickel metal used in beta filter. It is equipped with x-Celerator solid-state detector. Instrument operated using the 40 mA and 45 kV at a scanning speed of 5°/min. Below 200 mesh carbon powder sample was taken on glass side and collected the spectra. Thermal stability investigation of carbon samples was done by using TA Instruments Q500 thermogravimetric analyzer. Samples were analyzed in the temperature range from 20 to 950 °C with a heating rate 10 °C/min under atmosphere. 10 mg each sample was taken in the crucible and placed in the instruments.

3. Results and discussion

3.1. Studies on vacuum residue and ARA analysis

The vacuum residues exhibit distinct characteristics and hence there is significant variation in various fractions as shown in Fig. 2 extra heavy and heavy crude oil have an abundant asphaltene and resin fractions. Fig. 2 shows the results of ARA analysis from different regions. The range of resin and asphaltene fractions between origin based vacuum residues are 41.7–28.5 % and 27.9–2.4 %. Aromatic fraction ranges from 45 to 19.8 %, highest being LCO (45 %), followed by HCO (40.9 %) and least in EHCO (19.8 %). ARA fractions from LCO is aromatic rich whereas EHCO has the highest resin and asphaltene fractions. The data in Table 1 indicate the characteristics of vacuum residue (VR) from LCO, HCO and EHCO. As anticipated, extra heavy crude oil has high CCR,

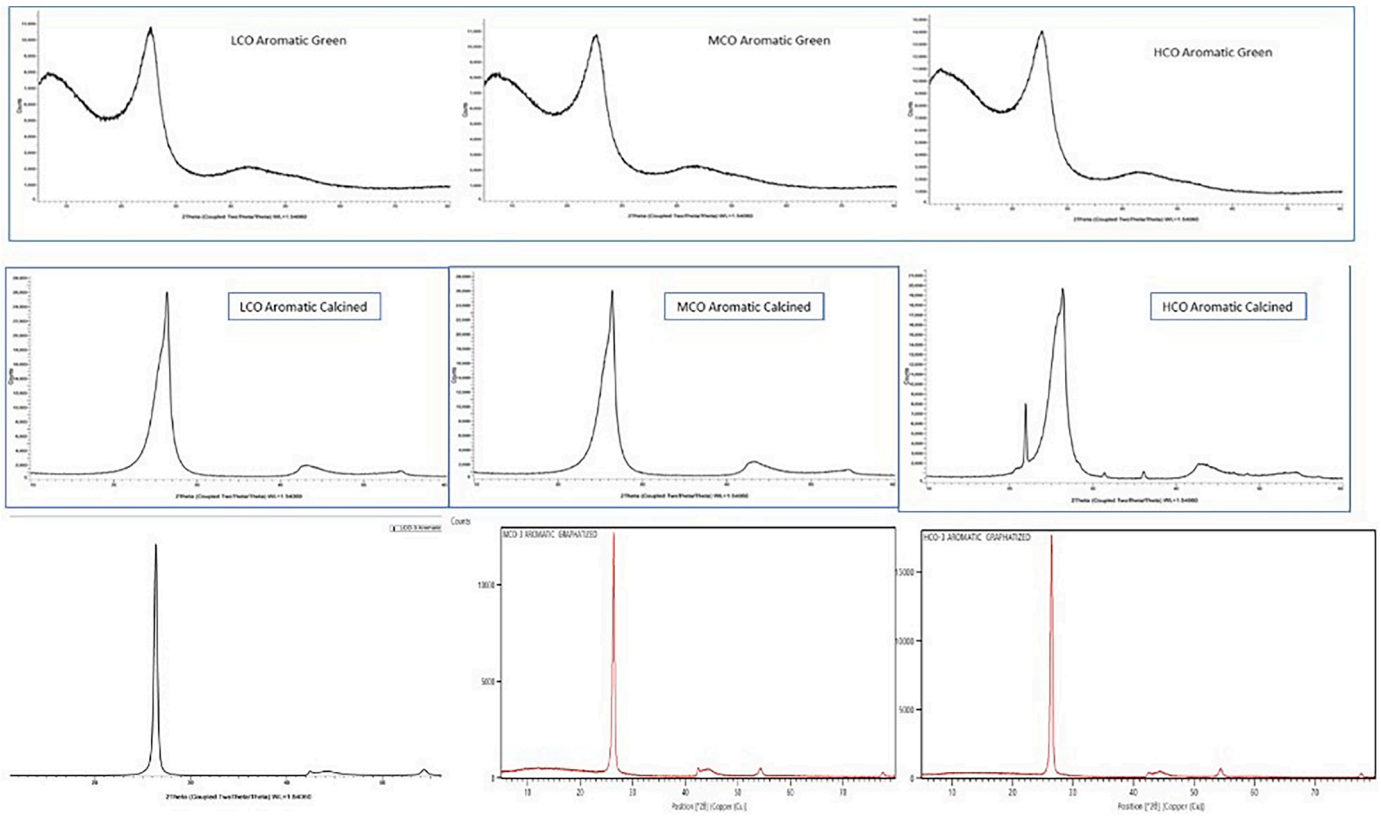

Fig. 12. XRD pattern of green, calcined and graphitized samples from aromatics.

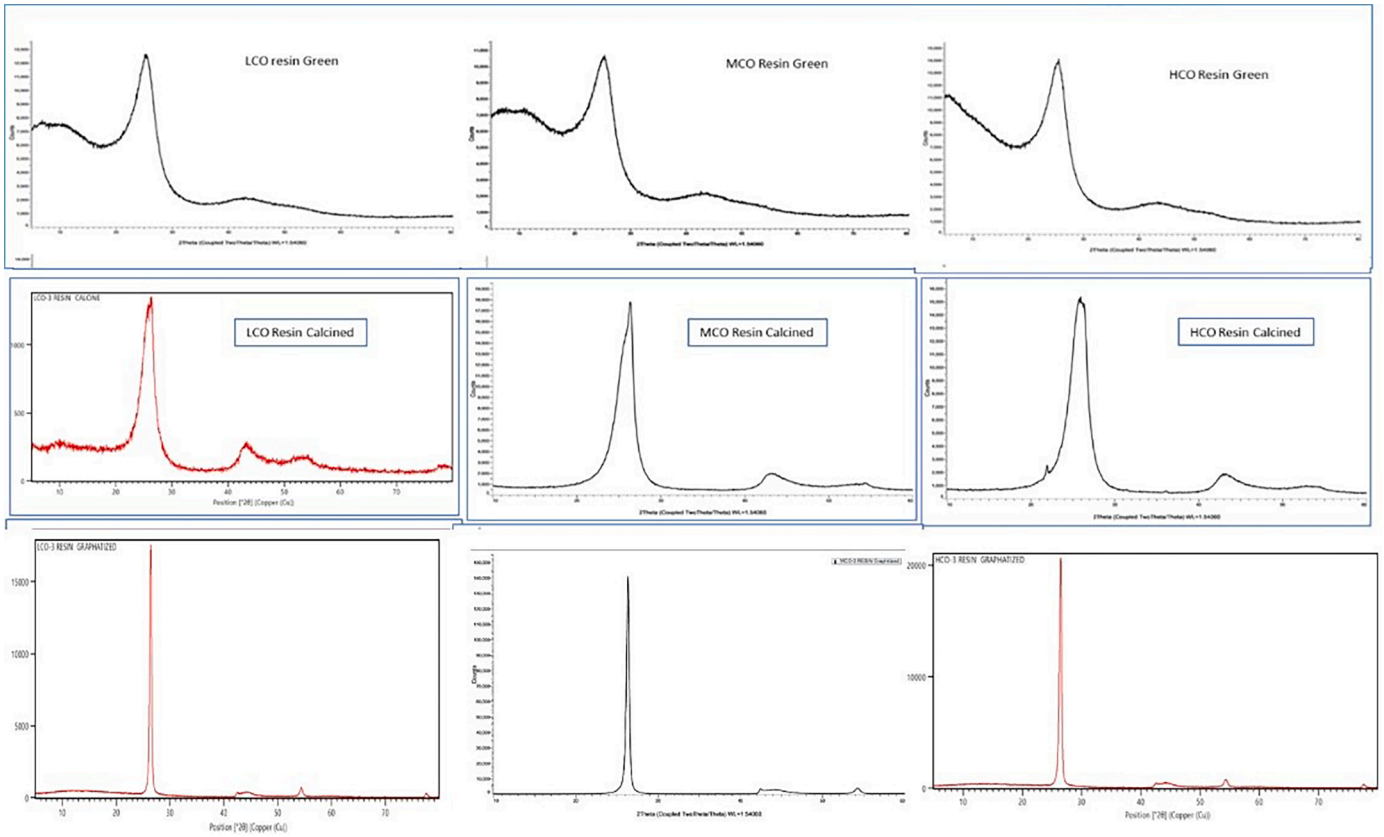

Fig. 13. XRD pattern of green, calcined and graphitized samples from resins.

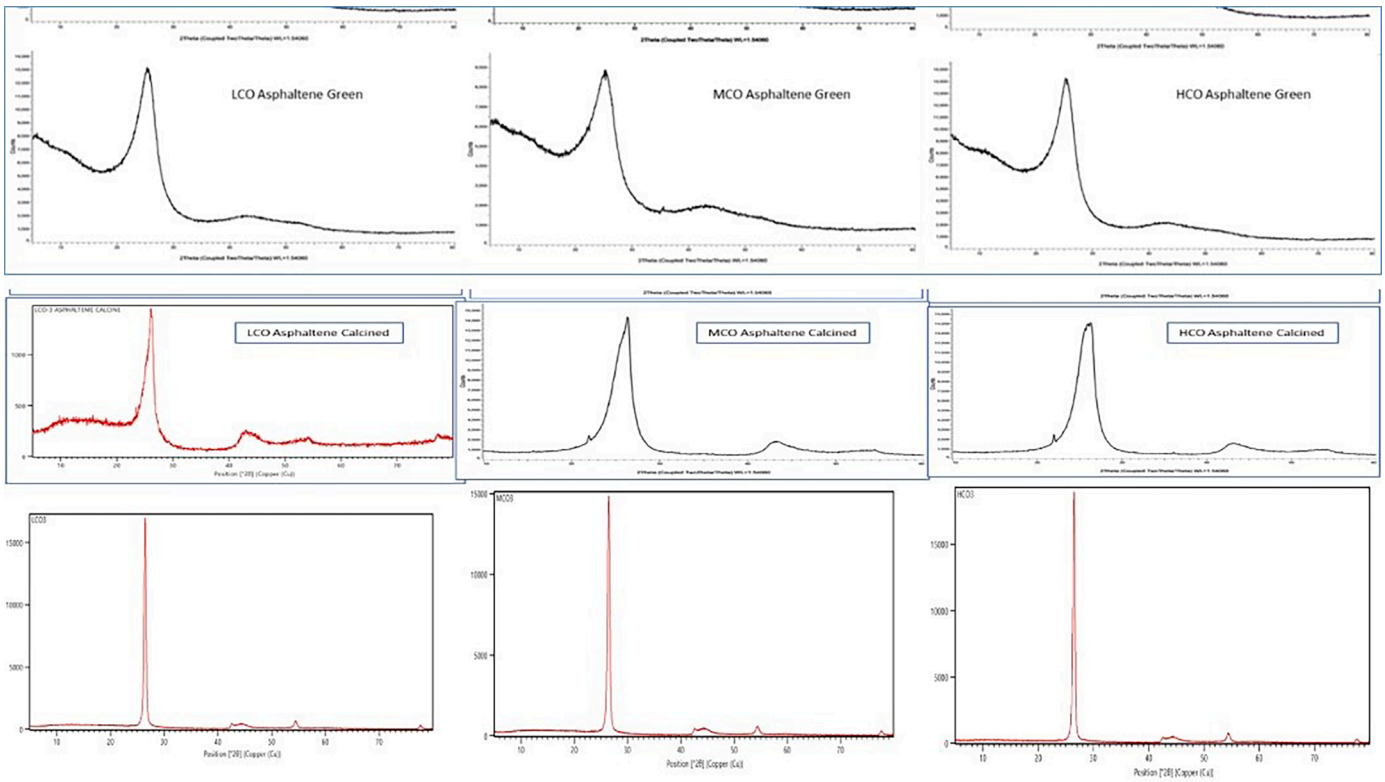

Fig. 14. XRD pattern of green, calcined and graphitized samples from asphaltenes.

pour point, density along with total carbon, nitrogen and metal. In contrast, heavy crude oil was found to be rich in total sulphur, oxygen, heteroatoms and high C/H ratio. Even though there is not any major dissimilarity in hydrogen content between origins, light crude oil has slightly high hydrogen content (11.2 %).

Fig. 3a to 3c shows TLC-FID chromatograms of the isolated ARA fraction from vacuum residue of (which sample LCO/HCO/EHCO). The chromatogram has distinct single peak representing 99 % purity and sufficient isolation. Density and CCR were used to predict ARA fractions of vacuum residues [39]. Fig. 3d summarizes the results of measurements of Conradson carbon content, which indicates the difference among the samples. For asphaltene and aromatic fraction, carbon content of EHCO dominates whereas that of LCO falls shortly behind EHCO. Further it is interesting to note that LCO preside over EHCO in resin fraction with slightly high carbon content. However, the carbon content of ARA fraction from HCO differs strongly with low value. Similarly, density is a key property for the assessment, simulation and expansion of petroleum reservoirs. Fig. 3e show the measured density for aromatic, resin and asphaltene from different origins. The light crude oil is a low-viscous material and is expected to have low density when compared to very viscous heavy/extra heavy oil with a high specific density [40]. However, it is interesting to note that the obtained value reflects the opposite trend (Fig. 3e). The density for LCO were found to be high in all the aromatic, resin and asphaltene fraction, respectively.

The elemental compositions of the investigated origin based ARA fraction are represented in Table 2. Regardless of the samples from different origin they are all carbon rich with more than 82 wt. % in ARA fractions. The carbon, hydrogen, C/H, nitrogen and oxygen composition of the aromatic fraction did not vary significantly irrespective of its origin. However, the sulfur and as a result the heteroatom content was high in aromatic fraction from HCO. The similar pattern was observed for the elemental composition in resin and asphaltene fractions. The elemental composition of carbon in the range of 80–90 % have been reported earlier for oils samples from south of Iran [27,4]. The H/C-ratio is an important guideline that indicates the degree of saturation and determines the abundance ratio of aromatic and aliphatic compounds. This ratio decreases with the increase in aromatic proportion and decrease in the aliphatic proportion. The H/C values of ARA below unity indicates the samples are highly aromatic [4]. The heteroatom content reached a maximum of approx. 8 wt. % in Asphaltene. Anyhow, sulfur was high in content among heteroatom in all ARA fractions. Aromatic fraction from LCO has the lowest sulfur (2.7 %) and oxygen (0.61 %), whereas from HCO has lowest nitrogen (0.39 %) content. Likewise, the high content of nitrogen (1.65 %), oxygen (0.61) and sulfur (8.34 %) were identified in asphaltene from EHCO and LCO, and resin fraction from HCO.

Inductively coupled plasma optical emission spectrometry are regularly used for crude oil and products analysis [16,41]. The ICP-OES results of ARA fractions shown in Fig. 4, illustrate the presence of metal and ash concentration in ARA fractions along with its variation among different origin sample. The metal concentrations in aromatic, resin and asphaltene are in the range of 39–204 ppm, 271–1233 ppm and 400–2154 ppm (Fig. 4a), respectively. The excess metal contents were present in ARA fractions from EHCO. The low metal content in LCO against HCO and EHCO agrees with the facts that light crude oil usually contains relatively low metal. The presence of metallic particles are important as they might have a significant role in the asphaltene accumulation [42]. Correspondingly (Fig. 4b), the ash concentration in aromatic, resin and asphaltene are in the range of 0.01–0.05 ppm, 0.07–0.39 ppm and 0.11–0.68 ppm. Consequently, the difference in ash content follow the same pattern noticed for metal concentrations.

Estimating molecular weight distribution of ARA fractions could be important to anticipate the phase behaviour and prevent asphaltene depositions. Similarly molecular weight distribution influences the chemical composition which directly affects the combustion characteristics of fuel oil [7]. Hence determination of molecular weight distribution becomes mandatory which is analysed by Gel Permeation chromatography in the present study. The number-average molecular weight (M_N) is defined as the average based on the number of polymer chain molecules at a particular molecular weight, whereas the

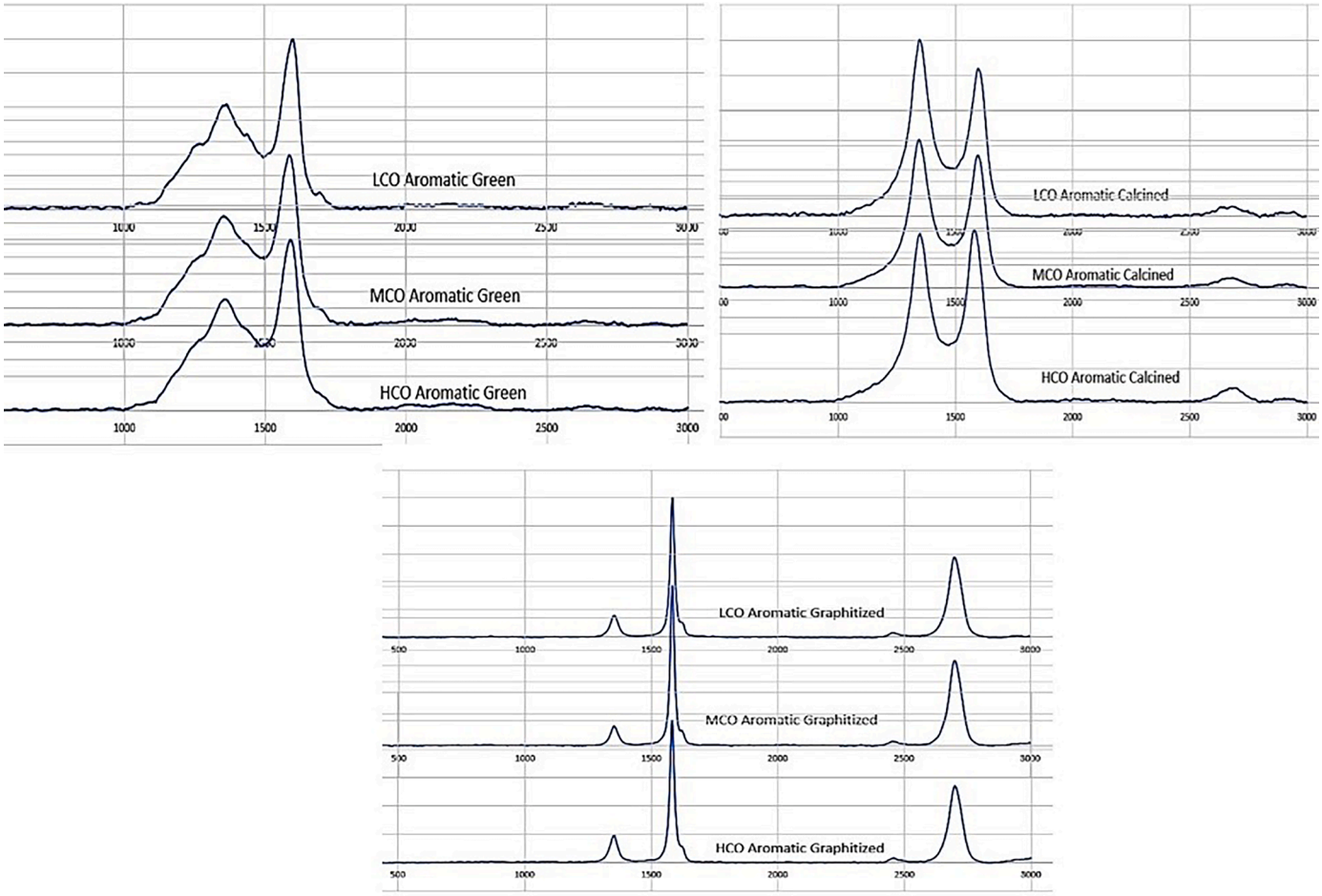

Fig. 15. Raman spectra of green, calcined and graphitized carbon of origin based aromatics.

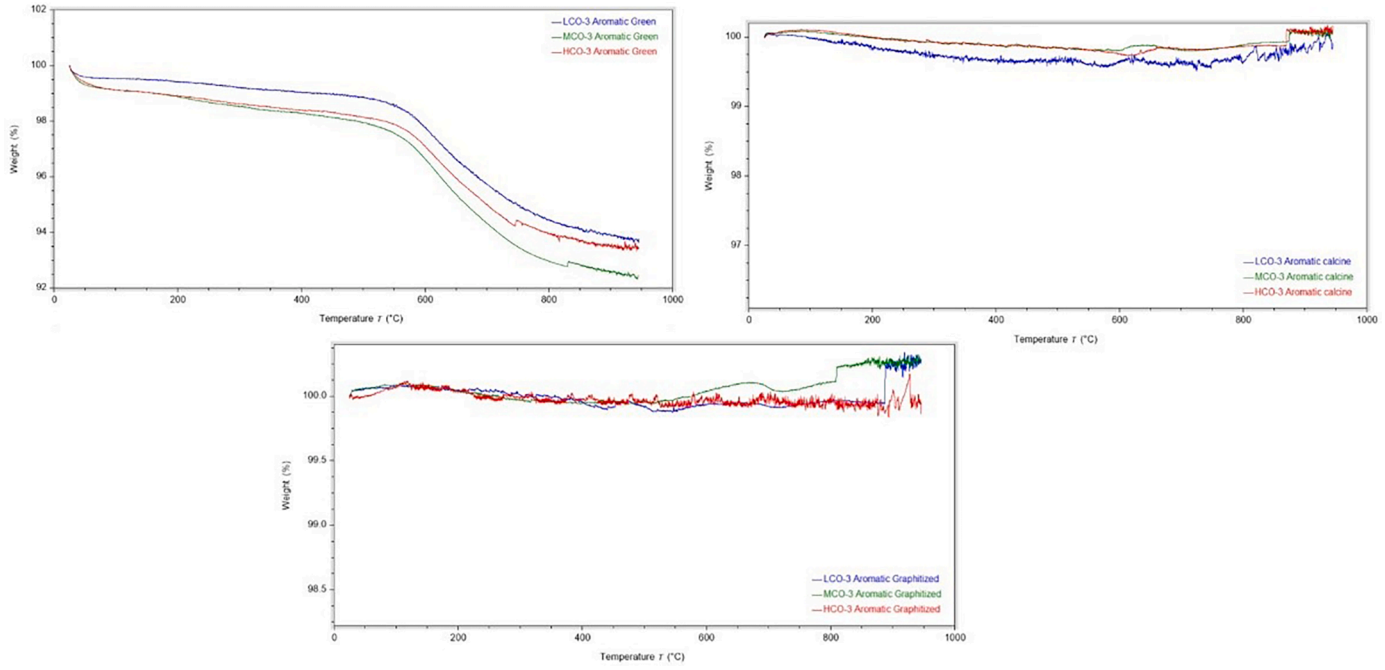

Fig. 16. TGA analysis of green, calcined and graphitized carbon from origin based ARA fractions.

Table 8
Data obtained for Raman analysis.

Sample	Origin	AROMATIC		RESIN		ASPHALTENE	
		I_D/I_G	La (nm)	I_D/I_G	La (nm)	I_D/I_G	La (nm)
Green	LCO	0.6164	31.19	0.6773	28.39	0.7175	26.79
	HCO	0.6424	29.92	0.6372	30.17	0.7454	25.79
	EHCO	0.6240	29.47	0.9220	27.77	0.6890	27.90
Calcined	LCO	1.1925	16.12	1.0112	19.01	1.2171	15.80
	HCO	1.1169	17.21	1.2641	15.21	1.2571	15.29
	EHCO	0.9812	19.59	1.2083	15.91	1.1948	16.09
Graphitized	LCO	0.1581	121.61	0.1241	154.95	0.1401	137.23
	HCO	0.1234	155.79	0.1552	123.84	0.4580	41.98
	EHCO	0.1902	101.07	0.1619	118.77	0.4149	46.34

weight-average molecular weight (MW) corresponds to the mass (or weight) of the polymer chain molecules at a particular molecular weight. Higher side poly dispersity indicates the broadness of molecule. As shown in Fig. 5a, the number-average molecular weight (M_N) of aromatics and resin were basically consistent with those of different origin. However, the M_N of asphaltenes derived from different origin were higher varying in the range of 2671–4850 ($g.mol^{-1}$). This proposed that the asphaltene especially derived from HCO had larger molecular weight with M_N value of 4850 ($g.mol^{-1}$). Likewise, the weight-average molecular weight (MW) for origin based ARA fractions based on GPC detection are shown in Fig. 5b. The results showed that there was great difference in MW for asphaltene compared with aromatic and resin fraction. The HCO-asphaltene had a high MW value of 21,845. Likewise the highest average molecular weight in asphaltene was presented by [6].

The polydispersity, an indication of heterogeneity of a sample based on size from the various fractions are illustrated in Fig. 5c. The values observed were very similar for the aromatic and resin fractions. Also it is has the same trend as its molecular weight distribution (Fig. 5a &b). G. A. Mansoori et al. [43] detected relative values of polydispersity for aromatic, resin and asphaltene from heavy fraction of crude oil by means of GPC. It is well reported fact that asphaltenes show a very large size polydispersity. The obtained results reflect the same result. Similarly, the asphaltene fraction has high polydispersity value as well it does not follow the trend noticed for molecular weight distribution. For instance, both mass and number molecular weight of asphaltene fraction follows the descending order of HCO, EHCO and LCO. But, for the polydispersity it follows a different order, where LCO has high value followed by HCO and EHCO. G. A. Mansoori et al. reports broad distribution of sizes and molecular characteristics for asphaltene [43]. D. Oldham et al. [44] investigated polydispersity of crude oil due to asphaltene oxidation and hypothesized that increased polydispersity affects viscosity.

Several researchers have published the application of NMR in the assessment of heavy petroleum fractions. The proton NMR spectroscopy is used for quantitative analysis of paraffinic and aromatic hydrogen, where carbon NMR spectroscopy is used for paraffinic and aromatic carbon atoms. For such complicated molecules, the aliphatic protons participation on a ^1H NMR spectrum emerges as a large signal with a continuous superimposing of numerous peaks and most strong compared to aromatics and are basically classified into three types of protons namely, a, b and c with reference to an aromatic core. The investigation of the range of every kind is not simple to attain but are commonly resolved from 0.1 to 1.1 ppm for d type protons, broad peck obtained at 1.2 to 2.1 ppm for c type protons, 6.0 to 7.1 ppm for b type protons and 7.0 to 9.0 for a type proton. Proton NMR provides type of hydrogen and its concentration in compound and also describe the nature of compound. Proton NMR attributed δ position of alkyl or paraffinic is 0.1 to 1.1 for methyl, 1.2 to 2.1 for aliphatic methylene and 2.2 to 4.0 for naphthenic or -CH, $-CH_2$ group proton. The aromatic proton resonance δ position for mono aromatic ring 6.0 to 7.1 and di. Tri and tetra or pera aromatic rings 7.3 to 9.0. Where $CDCl_3$ three peak appeared at 7.26 and TMS at 0. Table 3 shows the total aliphatic and aromatic proton. In aromatic, total aliphatic hydrogen increased from light to heavy and total aromatic hydrogen decreased from light to heavy. However, the similar contribution did not found in resins, where heavy crude resin have less aliphatic hydrogen and more aromatic hydrogen as compare to other resins fraction. Asphaltenes fraction have similarly to aromatic fraction aromatic proton increased from light to heavy and aromatic proton decreased from light to heavy. These results clearly signposted for aromatics and asphaltenes were light to extra heavy aromatic proton decreased and aliphatic proton increased however the resins did not follow the similar trend also C/H ratio in elemental analysis similar trend was derived Table 4.

The carbon skeleton was justified by the ^{13}C NMR which provided the structure information of carbon compound. For this reason, ^{13}CNMR spectra has turned to be a typical choice for the analysis of crude oil fractions. When comparing ^1H and^{13}C NMR spectra it is plausible to distinguish many variation between them. For instance, ^{13}C NMR spectra have huge chemical shifts scale (more than 220 ppm) that diminishes over lapping between peaks. The ^{13}C NMR is insensible than ^1H NMR because of its reduced natural abundance and magnetogyric ratio of the^{13}C nucleus, but in the event of the ^1H decoupled ^{13}C NMR spectra it is more straightforward when there is no peak splitting. The ^{13}C NMR signals between 20.00 and 40.00 ppm come from aliphatic of -CH and $-CH_2$ associated to linear alkanes and cyclic compounds. The methyl group have ^{13}C NMR signals have 10 to 20 with braches methyl group also appeared in this range. While aromatic carbon showed the signal in ^{13}C NMR between 110 and 160 ppm. Above table represent the aromatic carbon increasingly pattern showing from light to heavy. However, the total carbon lowers side in HCO fractions matrix due to higher side hetero atoms.

3.2. Preparation of graphitic carbon like material

The heat treatment of ARA fractions were carried out in different stages. The products obtained at various stages of heat treatment of ARA fraction were referred as green (stage I), calcined (stage II) and graphitized carbon (stage III). In order to obtain green coke, the ARA fraction was used as raw material. Table 5 shows the yield of carbon at different stages of pyrolysis. The highest yield of green carbon for ARA fractions was noticed for EHCO, except for resin fractions where LCO has more yield. However the lowest yield of green carbon for ARA fractions was from MCO. The yield of green carbon was in the range of 15.4–23.3, 31.4–41.5 and 52–65 for aromatic, resin and asphaltene fractions. The yield of calcined carbon denotes more conversion has taken place for aromatic and resin fraction when compared to asphaltene. The yield of calcined carbon did not show much variation among ARA fraction and is in the range of 71.5–85. Moreover, the yield of graphitized carbon for all ARA fraction are above 90. Almost complete conversion has taken place for aromatic (EHCO) and asphaltene (HCO) which is 99.3 and 99.5.

The effect of pyrolysis temperature on elemental content is presented in Table 6. Table 6 shows that carbon content increases on calcination and graphitization of green carbon. At the same time, as expected there was a progressive decrease of hydrogen, nitrogen, sulphur and oxygen

with calcination and graphitization process corresponding to an increase of volatile and gases (CO, CO_2, NO_2, CH_4) loss [45]. The decrease of oxygen is anticipated to increase the sample basic nature [46]. Hence, the increased C/H and C/O ratios are indicative of dehydrogenative polymerization and dehydrative polycondensation during heat treatment [45]. Further, the relatively high quantities of heteroatoms in green carbon decreases on calcination and graphitization showing the loss of numerous functional groups [45]. The highest amount of carbon (99.99) in all ARA fractions after graphitization process indicates the complete graphitization.

Fig. 6 shows the thermogravimetric analysis of green, calcined and graphitized samples of ARA fractions. The TGA curve of green aromatic fraction represented three decomposition stages. However the overall weight loss was only 7 %. The first weight loss step started at about 27.8 °C, was related to adsorbed moisture and impurities. While the second weight loss step initiated at about 554.28 °C may be attributed to the reaction of carbon with oxygen leading to the release of CO_2 [47]. The third weight loss step at around 727 °C may be to the sublimation of carbon backbone [48]. The TGA curve of calcined and graphitized aromatic fraction shows negligible weight loss indicating the thermal stability of the formed graphite. The characteristics were identical for resin and asphaltene fractions.

The XRD patterns of the green, calcined and graphitized origin based aromatic fraction are shown in Fig. 7. A difference in XRD pattern was noticed, green carbon exhibited broad peak at approximately $2\theta = 25.46^\circ$ with low intense shoulder peak at around $2\theta = 43.24^\circ$. These corresponds to the (002) and (004) peaks indication presence of some less oriented graphitic carbon in samples. XRD patterns of calcined samples show increase in intensity of peak with shifting towards higher theta values this indicates more orientation of carbon atoms in graphitic manner. Further on graphitization the peak turns completely symmetric with a sharp peak representing the presence of only graphitic carbon like material in samples. This shows the formation of graphitic carbon like material from cured derived carbon at high temperature. The HCO and EHCO fractions (Figs. 8and 9) for green, calcined and graphitized represents the same behavior comparative to aromatic fraction as shown in Fig. 7, except for a small change. In case of calcined HCO, there is an additional sharp peaks at $2\theta = 21.86^\circ$, 31.54° and 36.25°. Even for resin and asphaltene fraction, the XRD patterns show same behavior as observed in aromatic fraction for all green, calcined and graphitized process.

The interlayer spacing obtained from the XRD patterns are given in Table 7. The interlayer spacing of green carbon were around the range 3.505–3.538 Å, this indicates presences of less oriented graphitic carbon in starting material. Moreover, the interlayer spacing of calcined and graphitized carbon decreases to around 3.36 Å indicating the formation of highly ordered graphitic carbon after high temperature treatment to graphite like material. In addition the crystallite size L_a and L_c were calculated to assess the average size of the carbon atoms. In the green sample, the L_c and L_a were in the range 19.90–24 Å and 16.90–25.30 Å which shows a notable decrease on calcination indicating the increase of defects in the structure. Further, with graphitization there was once again a remarkable increase in Lc and La values suggesting the increase of order with the transformation to graphite like structure. There was not any distinguishable difference in interplanar spacing and crystallite size with feed quality variation due to ARA fraction from different origin Figs. 10–16.

The transformation to graphite like material in the samples has been further supported by Raman spectroscopy. In the recent years, pyrolysis of petroleum vacuum residue is procuring significant recognition with raising awareness on sustainability, the transformation and nature of carbonaceous substance were analyzed in depth with the aid of Raman spectroscopy [49]. As shown inFig. 12, the Raman spectrum of carbon from origin based aromatics exhibits two peaks at 1355 $cm^{-1}$and 1575 cm^{-1}, which are designated to the D band and G band, correspondingly. These peaks grow sharp and intense on calcination, indicating the orientation of carbon atoms in more ordered way. Additionally, a broad peak evolves around 2500 cm^{-1} denoting the coexistence of graphite phase. With the further increase in temperature during graphitization process, the Raman spectrum exhibits defect (D) and graphitic (G) bands at 1354 and 1584 cm-1 and an overtone 2D band at about 2716 cm-1, reflecting the transformation of highly crystalline graphitic material. The Raman spectra of other samples particularly origin based along with ARA fraction reveal similar patterns irrespective of different feed quality.

The ratio of I_D/I_G estimated for the studied specimens are denoted in Table 8. While the G-band is produced by the C—C stretching and exists in all carbon structures, the d-band evolves from the breathing mode of aromatic rings [50]. The d-band indicates presence of disorder carbon in material. The intensity ratio of the D and G band (I_D/I_G) may thus be an indirect assessment of the disorder within the sample. The I_D/I_G value for the ARA fraction of the green sample were in the range 0.6164–0.6890, representing disordered structure. Slightly higher I_D/I_G values were noted for graphitized resin as well green and calcined asphaltene. The I_D/I_G value once again increases which later decreases with increase in temperature, indicating the changes in arrangement of carbon within the material from random to highly ordered carbon like graphitic carbon.

4. Conclusion

The characteristics of LCO, HCO and EHCO crudes and their vacuum residual fractions i.e. feed quality are varying significantly due to effect of different origin. These three crudes vacuum residues and their fractions exhibited an ascending trend in terms of both total metals percentage and ash %, with the lighter fractions having lower values and the heavier fractions having higher values. The HCO aromatic fractions have a larger presence of heteroatoms and aliphatic protons (-CH_3, -CH_2) as observed directly through ^{1}H NMR and ^{13}C NMR. ARA fractions were explored as a sustainable precursor to produce graphitic carbon like materials. The incomplete conversion for green carbon were revealed by several decomposition stages during TGA studies. Both XRD and Raman indicate that graphitic carbon like material was successfully synthesized from aromatic, resin and asphaltene fraction via the pyrolysis and high temperature treatment of cured derived carbon. The results of XRD revealed that the diffraction lines at $2\theta = 25.46^\circ$, and the interlayer spacing of green carbon were in the range 3.505–3.538 Å, and subsequent reduction with high temperature treatment to 3.38 Å which shows formation of high ordered graphitic carbon. Likewise, the Raman spectrum of green carbon exhibits presence of D band at 1355 $cm^{-1}$and G band at 1575 cm^{-1} that supports the presence of graphitic carbon. The intensity ratio of the D and G band (I_D/I_G) from Raman spectra confirmed the transformation of present amorphous like carbon to highly ordered graphitic carbon after high temperature treatment. Further, the thermal stability of the calcined and graphitized carbon have been proven by TGA analysis. The XRD, Raman and TGA of the samples determined no difference irrespective of different feed quality for the preparation of graphitic carbon like material from cured based carbon.

CRediT authorship contribution statement

Ravi Dalsania: Writing – original draft, Validation, Supervision, Methodology, Investigation, Formal analysis. **Hasmukh Gajera:** Writing – review & editing, Supervision, Project administration, Investigation, Data curation, Conceptualization. **Mahesh Savant:** Writing – review & editing, Supervision, Project administration, Conceptualization.

Declaration of competing interest

The authors declare the following financial interests/personal

relationships which may be considered as potential competing interests: Ravi Dalsania reports administrative support was provided by Atmiya University. Ravi Dalsania reports a relationship with Reliance Industries Ltd that includes: employment. If there are other authors, they declare that they have no known competing financial interests or personal relationships that could have appeared to influence the work reported in this paper.

Acknowledgments

The authors thank Dr. Harender Bisht (the Geological Survey of Namely Light crude oil (LCO) from Middle East, Middle crude oil (MCO) from Canada and Heavy crude oil (HCO) from South America respectively) for helpful discussions. This work was supported by Reliance industries Ltd, India.

Data availability

Data will be made available on request.

References

[1] N.A. Alawani, S.K. Panda, A.R. Lajami, T.A. Al-Qunaysi, H. Muller, Characterization of crude oils through alkyl chain-based separation by gel permeation chromatography and mass spectrometry, Energy Fuels 34 (2020) 5414.
[2] D. Stratiev, I. Shishkova, I. Tankov, A. Pavlova, Challenges in characterization of residual oils. A review, J. Petroleum Science and Engineering 178 (2019) 227.
[3] J. Sainbayar, D. Monkhoobor, B. Avid, Determination of trace elements in the tamsagbulag and tagaan els crude oils and their distillation fractions using by ICP-OES, Advances in Chemical Engineering and Science 2 (2012) 113.
[4] A.R.S. Nazar, L. Bayandory, Investigation of asphaltene stability in the iranian crude oils, Iranian J. Chem. Eng. 5 (2008).
[5] T.V. Le Doan, N.W. Bostrom, A.K. Burnham, R.L. Kleinberg, A.E. Pomerantz, P. Allix, Green river oil shale pyrolysis: semi-open conditions, Energy Fuels 27 (2013) 6447.
[6] M. Nikookar, M.R. Omidkah, G.R. Pazuki, A.H. Mohammadi, An insight into molecular weight distributions of asphaltene and asphalt using Gel Permeation Chromatography, J. Mol. Liq. 362 (2022) 119736.
[7] S.L.S. Sarowha, Determination of molecular weights of petroleum products using gel permeation chromatography, Pet. Sci. Technol. 23 (2005) 573.
[8] B. Azinfar, M. Zirrahi, H. Hassanzadeh, J. Abedi, Characterization of heavy crude oils and residues using combined Gel Permeation Chromatography and simulated distillation, Fuel 233 (2018) 885.
[9] M. Makowska, T. Pellinen, Thin layer chromatography performed in stages to identify the presence of aromatic like fraction in chosen bitumen modifiers, J. Traffic and Transport. Eng. 8 (2021) 453.
[10] D.A. Karlsen, S.R. Larter, Analysis of petroleum fractions by TLC-FID: applications to petroleum reservoir description, Org. Geochem. 17 (1991) 603.
[11] H.S. Bisht, M. Reddy, M.A. Malvanker, R. Patil, A. Gupta, B. Hazarika, A. Das, Efficient and quick method for saturates, aromatics, resins, and asphaltenes analysis of whole crude oil by thin-layer chromatography–flame ionization detector, Energy Fuels 27 (2013) 3006.
[12] S.A. Khan, S. Sarfraz, D. Price, TLC-FID calibration and accurate weight determination of SARA fractions in heavy crude oil, Pet. Sci. Technol. 30 (2012) 2401.
[13] M.A. Azam, N.E. Safie, H.H. Hamdan, Effect of sulfur content in the crude oil to the corrosion behaviour of internal surface of API 5L X65 petroleum pipeline steel, Manuf. Technol. 21 (2021) 561.
[14] G.H.C. Prado, Y. Rao, A.D. Klerk, Nitrogen removal from oil: a Review, Energy Fuels 31 (2017) 14.
[15] C.E. Chukwuneke, J.O. Madu, B.O. Agboola, Determining ash content and trace metal concentration in crude oil samples to teach students sample preparation and instrumental analysis, J. Chem. Educ. 98 (2021) 633.
[16] J.S. Mandlate, A.S. Henn, P.A. Mello, E.M.M. Flores, J.S. Barin, F.A. Duarte, Determination of Cl and S in crude oil by ICP-OES after sample digestion by microwave-induced combustion in disposable vessels, Anal. Chim. Acta 1273 (2023) 341536.
[17] F. Low, L. Zhang, Microwave digestion for the quantification of inorganic elements in coal and coal ash using ICP-OES, Talanta 101 (2012) 346.
[18] A. Saydut, Microwave acid digestion for the determination of metals in subbitumnious coal bottom ash by ICP-OES, Energy Explor. Exploit. 28 (2010) 105.
[19] J.M. Santos, A. Vetere, A. Wisniewski Jr, M.N. Eberlin, W. Schrader, Comparing crude oils with different api gravities on a molecular level using mass spectrometric analysis. Part 2: resins and asphaltenes, Energies 11 (2018) 2767.
[20] J.P. Arenaz-Diaz, D.C. Palacio, C.X. Ramirez, R. Cabanzo, A. Guzman, E. Mejia-Ospino, Chemical characterization of polar species in colombian vacuum residue and its supercritical fluid extraction subfractions using electrospray ionization FT-ICR mass spectrometry, Chem. Eng. Transact. 57 (2017) 2283.
[21] Z. Farmani, W. Schrader, A detailed look at the saturate fractions of different crude oils using direct analysis by ultrahigh resolution mass spectrometry (UHRMS), Energies 12 (2019) 3455.
[22] M. Pudenzi, N. Eberlin, Assessing relative electrospray ionization, atmospheric pressure photoionization, atmospheric pressure chemical ionization, and atmospheric pressure photo- and chemical ionization efficiencies in mass spectrometry petroleomic analysis via pools and pairs of selected polar compound standards, Energy Fuels 30 (2016) 7125.
[23] A. Wick, G. Fink, T.A. Ternes, Comparison of electrospray ionization and atmospheric pressure chemical ionization for multi-residue analysis of biocides, UV-filters and benzothiazoles in aqueous matrices and activated sludge by liquid chromatography–tandem mass spectrometry, J. Chromatogr. 1217 (2010) 2088.
[24] A.K. Huba, K. Huba, P.R. Gardinali, Understanding the atmospheric pressure ionization of petroleum components: the effects of size, structure, and presence of heteroatoms, Sci. Total Environ. 568 (2016) 1018.
[25] I. Zojaji, A. Esfandiarian, J. Taheri-Shakib, Toward molecular characterization of asphaltene from different origins under different conditions by means of FT-IR spectroscopy, Adv. Colloid Interface Sci. 289 (2021) 102314.
[26] N. Esmaeilian, N. Rabiei, M. Mahmoudi, B. Dabir, Asphaltene structure determination: FTIR, NMR, EA, ICP-OES, MS, XRD and computational chemistry considerations, J. Moleccul. Liquids 385 (2023) 122279.
[27] M. Asemani, A.R. Rabbani, Detailed FTIR spectroscopy characterization of crude oil extracted asphaltenes: curve resolve of overlapping bands, J. Pet. Sci. Eng. 185 (2020) 106618.
[28] S.B. Yang, J. Moreira, Z. Li, Predicting crude oil properties using fourier-transform infrared spectroscopy (FTIR) and data-driven methods, Digital Chem. Eng. 3 (2022) 100031.
[29] G. Gao, J. Cao, T. Xu, H. Zhang, Y. Zhang, K. Hu, Nuclear magnetic resonance spectroscopy of crude oil as proxies for oil source and thermal maturity based on 1H and13C spectra, Fuel 271 (2020) 117622.
[30] T.F. Canan, S. Ok, W. Al-Bazzaz, S. Ponnuswamy, M. Fernandes, M. Al-Shamali, A. Qubian, A. Sagidullin, Rapid characterization of crude oil by NMR relaxation using new user-friendly software, Fuel 320 (2022) 123793.
[31] I. Rakhmatullin, S. Efimov, V. Tyurin, M. Gafurov, A. Al-Muntaser, M. Varfolomeev, V. Klochkov, Qualitative and quantitative analysis of heavy crude oil samples and their SARA fractions with 13C nuclear magnetic resonance, Processes 8 (2020) 995.
[32] D. Stratiev, I. Shiskova, V. Toteva, G. Georgiev, R. Dinkov, I. Kolev, I. Petrov, G. Argirov, V. Bureva, S. Ribagin, K. Atanassov, S. Nenov, S. Sotirov, Experience in processing alternative crude oils to replace design oil in the refinery, Resources 13 (2024) 86.
[33] A.B. Garmarudi, M. Khanmohammadi, H.G. Fard, M. Guardia, Origin based classification of crude oils by infrared spectrometry and chemometrics, Fuel 236 (2019) 1093.
[34] O. Galtier, O. Abbas, Y. Dreau, C. Rebufa, J. Kister, J. Artaud, N. Dupuy, Comparison of PLS1-DA, PLS2-DA and SIMCA for classification by origin of crude petroleum oils by MIR and virgin olive oils by NIR for different spectral regions, Vib. Spectrosc. 55 (2011) 132.
[35] M. Salehzadeh, M.M. Husein, C. Ghotbi, B. Dabir, V. Taghikhani, In-depth characterization of light, medium and heavy oil asphaltenes as well as asphaltenes subfractions, Fuel 324 (2022) 124525.
[36] X. Zhai, W. Lin, J. Liu, X. Chen, J. Yong, W. Yang, Fe_3C/Fe, N-codoped porous carbon from petroleum vacuum residual for highly efficient oxygen reduction, J. Electroanal. Chem. 866 (2020) 114170.
[37] J.L. Tirado, R. Santamaria, G.F. Ortiz, R. Menendez, P. Lavela, J.M. Jimenez-Mateos, F.J.G. Garcia, A. Concheso, R. Alcantara, Tin–carbon composites as anodic material in Li-ion batteries obtained by copyrolysis of petroleum vacuum residue and SnO_2, Carbon N Y 45 (2007) 1396.
[38] H. Chao, J. Liu, Preparation of the 3D porous carbon based on vacuum residue and its application in lithium ion capacitors, J. Phys.:Conf. Ser 2044 (2021) 012117.
[39] K.H. Lim, S. Kim, H. Kweon, S. Moon, C.H. Lee, H. Kim, Preparation of graphene hollow spheres from vacuum residue of ultra-heavy oil as an effective oxygen electrode for Li–O_2 batteries, J. Mater. Chem. A 6 (2018) 4040.
[40] M. Paliukaite, A. Vaitkus, A. Zofka, Evaluation of bitumen fractional composition depending on the crude oil type and production technology, in: The 9th international conference "Environmental Engineering, 2014.
[41] T.R. Penha, J.R. Almeida, R.M. Sousa, E.V.R. Castro, M.T.W.D. Carneiro, G. P. Brandao, Multielement analysis of crude oil produced water by ICP OES after acid digestion assisted by microwave, J. Anal. At. Spectrom. 30 (2015) 1154.
[42] A.C.S. Berna, V.C. Moran, E.T.R. Guzman, M.J. Yacaman, Asphaltene aggregation from vacuum residue and its content of inorganic particles, Pet. Sci. Technol. 24 (2013) 1055.
[43] G.A. Mansoori, D. Vazquez, M.S. Niassar, Polydispersity of heavy organics in crude oils and their role in oil well fouling, J. Petroleum Science and Engineering 58 (2007) 375.
[44] D. Oldham, X. Qu, H. Wang, E.H. Fini, Investigating change of polydispersity and rheology of crude oil and bitumen due to asphaltene oxidation, Energy Fuels 34 (2020) 10299.
[45] C.O.E. Eromosele, C.N. Onwucha, S.O. Ajayi, G. Melinte, A.L. Hansen, S. Indris, H. Ehrenberg, Ionothermal preparation of activated carbon from waste PET bottles as anode materials for lithium ion batteries, RSC Adv. 12 (2022) 34670.
[46] P.D. Filippis, L.D. Palma, E. Petrucci, M. Scarsella, N. Verdone, Production and characterization of adsorbent materials from sewage sludge by pyrolysis, Chem. Eng. Transact. 32 (2013) 1974.

[47] A.D. Jara, G. Woldetinsae, A. Betemariam, J.Y. Kim, Mineralogical and petrographic analysis on the flake graphite ore from Saba Boru area in Ethiopia, Int. J. Mining Sci. Technol. 30 (2020) 715.
[48] S.N. Alam, N. Sharma, L. Kumar, Preparation of Graphene Oxide (GO) by modified hummers method and its thermal reduction to obtain reduced graphene oxide (rGO), Graphene 6 (2017) 1.
[49] Z. Zhang, Q. Wang, The new method of XRD measurement of the degree of disorder for anode coke material, cryst. 7 (2017) 5.
[50] V. Scardaci, G. Compagnini, Raman spectroscopy investigation of graphene oxide reduction by laser scribing, J. Carbon Res. 7 (2021) 48.